PRESSURE AND VELOCITY DISTRIBUTION FOR AIR FLOW THROUGH FRUITS PACKED IN SHIPPING CONTAINERS USING POROUS MEDIA FLOW ANALYSIS

M.T. Talbot, Ph.D., P.E. **C.C. Oliver, Ph.D., P.E.** **J.J. Gaffney, P.E.**
Member ASHRAE

ABSTRACT

A commercial finite element solution package was used to determine pressure and velocity distributions of air flow through a three-dimensional orange carton using a porous media flow analysis. To verify the porous media analysis for this problem, an indirect method of comparison was developed. Temperature was measured for 12 different test conditions during cooling of oranges packed in an experimental orange carton. An existing heat transfer model was modified to incorporate the calculated velocity distribution and provided a predicted temperature response. The experimental and predicted temperature responses for the 12 tests were compared and this comparison was used to indirectly evaluate the flow information calculated by the porous media flow analysis. Although several areas for improvement were noted, the porous media flow analysis was found to provide adequate information if variable porosity within the orange carton was considered.

INTRODUCTION

Losses of fresh fruits and vegetables and other horticultural commodities from decay and shriveling as a result of poor temperature management during postharvest handling, transportation, and marketing are substantial in the United States and in other production and consumption areas of the world. Temperature is the most important environmental factor that influences the deterioration rate of harvested commodities. Handenburg et al. (1986) reported the rate of deterioration increases two- to threefold for each increase of 18°F (10°C) above the optimum temperature. Thus, improved cooling of fruits and vegetables before or during shipment, along with proper temperature maintenance throughout the marketing channels, has the potential to greatly reduce these losses.

Nearly all fresh fruits and vegetables are now marketed in corrugated fiberboard shipping containers. These containers provide a barrier to proper air flow and efficient heat transfer required for cooling. Industry sources recognize the need for additional research on air movement during cooling of fruits and vegetables in palletized shipments.

To understand and model heat transfer during cooling and storage of fresh fruits and vegetables packed in fiberboard shipping containers, the pressure and velocity field characteristics within the container must be established. Both distributions are difficult to establish experimentally. Many interrelated variables are involved during air cooling of fruits and vegetables. These include thermal properties, physical properties, and size and shape of the product, as well as temperature, flow rate, and relative humidity of the cooling air. When cooling products in containers, other important variables are container size, shape, and wall thickness; venting and stacking arrangements; product packing configurations; and airflow direction.

The objectives of this study were to (1) determine the feasibility of the theory of flow through porous media analysis for finite boundary conditions of air flow through fresh fruits and vegetables packed in shipping containers, (2) use a commercial finite element model to predict air pressure and velocity distribution for air flow through fruits packed in fiberboard packing containers, and (3) evaluate the predicted cooling response determined using the mathematical flow model in conjunction with an existing heat transfer model.

Fluid Flow Through Porous Media

The basis of nearly all engineering calculations for porous media flow problems have originated from Darcy's Law and/or purely empirical findings (Collins 1961; Muskat 1946; Scheidegger 1960). Darcy's Law is written as:

$$Q = kA\Delta h/\Delta L \quad (1)$$

Dividing both sides by the cross-sectional area, A, yields

M.T. Talbot, Assistant Professor, Agricultural Engineering Department, and **C.C. Oliver,** Professor, Mechanical Engineering Department, University of Florida; and **J.J. Gaffney,** Agricultural Engineer, USDA, ARS, Gainesville, FL.

$$V_s = k\Delta h/L \quad (2)$$

where

Q = flow rate in volume per unit time
k = permeability or hydraulic conductivity
Δh = pressure loss or head
ΔL = length of the flow path
V_s = superficial velocity.

Later investigators found that application of Darcy's Law is limited to very low velocity (creep) flow and becomes invalid when inertial forces become effective. Since then, several related theories and approaches have been developed to approximate the flow of fluid through porous media.

Based on Reynolds' theory for resistance to fluid flow, Ergun (1952) illustrated that pressure drop through porous media is caused by the simultaneous viscous and kinetic energy losses. A general equation for fluid flow through porous media was developed:

$$\Delta P/\Delta L = 150\mu V_s(1 - \epsilon)^2/D_p^2\epsilon^3 + 1.75\rho V_s^2(1 - \epsilon)/D_p\epsilon^3 \quad (3)$$

where

ΔP = pressure loss
μ = fluid viscosity
ϵ = porosity = void volume/total volume
D_p = mean diameter of particles of the porous material
ρ = fluid density

In terms of dimensionless groups, the Ergun equation can be written as:

$$\Delta PD_p\epsilon^3/\Delta L\rho V_s^2(1 - \epsilon) = 150\mu(1 - \epsilon)/\rho V_s D_p + 1.75 \quad (4)$$

In three-dimensional form, Equation 3 may be written as follows:

$$-\partial P/\partial x_i = f_1 V_i + f_2 V_i^2 \quad (5)$$

where

x_i = x, y, and z rectangular coordinates
$\partial P/\partial x_i$ = pressure gradient decreasing along positive x_i direction
V_i = velocity in x, y, and z directions
f_1 = $150\mu(1 - \epsilon)^2/D_p^2\epsilon^3$
f_2 = $1.75\rho(1 - \epsilon)/D_p\epsilon^3$

Another modification of Darcy's Law that has received considerable attention is a simplified, semi-empirical approach to account for nonlinear flow patterns of air through porous media. This is accomplished by assuming air velocity proportional to the pressure gradient raised to a power. Shedd (1953) introduced the following equation in the study of air flow through grain storages:

$$V = A(\partial P/\partial n)^B \quad (6)$$

where

V = interstitial fluid velocity
$\partial P/\partial n$ = pressure gradient along any direction
A,B = experimentally determined constants.

One major difference between Equation 6 and Equation 3 is the absence of porosity, which is assumed to be lumped with other characteristic properties of the fluid and porous medium into constants A and B.

Talbot (1987) reported on numerous research studies of the cooling, heating, and drying of semi-infinite systems of bulk-piled agricultural products such as fruits, grains, vegetables, nuts, and root crops using the theory of fluid flow through porous media to determine the pressure and velocity fields. This extensive theory of porous media flow for the study of air flow through agricultural commodities was generally classified into three areas of study. The first area is a development of equations for prediction of pressure drop as a result of air flow through bulk fruits and vegetables. The second is the prediction of pressure and velocity field distributions for air flow through bulk agricultural products. The third, and most limited, area of study is the development of equations to predict the pressure drop for air flow through fruits and vegetables packed in shipping containers. Wang and Tunpun (1969) studied the pressure drop vs. airflow relationships for tomatoes in bulk and in cartons. Haas et al. (1976) used a modified Shedd equation to develop relationships between pressure drop and air velocity for oranges in bulk and in cartons. Chau et al. (1983) used both the Shedd and Ergun equations to predict the pressure drop as a function of air flow for oranges in bulk and in cartons. No studies exist which predict pressure and flow fields through fruits or vegetables packed in containers.

EXPERIMENTAL TEMPERATURE MEASUREMENT

Direct measurement of air pressure and velocity within the packed carton is not feasible with current instrumentation. The measurement of temperature is the best direct method that can be used as an indication of the velocity pattern of the air passing through the carton as the product is cooled.

Experimental Orange Carton

The physical problem selected for modeling an individual carton packed with oranges, using porous media flow analysis, was an experimental box approximately the size of a commercial packing container used for oranges. The experimental box, shown in Figure 1, was constructed of 3/4 in. (1.8 cm) plywood with a lining of 3/4 in. (1.8 cm) insulation board and interior dimensions of 15 by 11 by 11 in. (38.1 by 27.9 by 27.9 cm). The box was constructed with 10 air vents, which allowed analysis of various airflow patterns through the box of oranges during cooling. The air vents were constructed by drilling holes in the box at the desired locations, as indicated in Figure 1. Using threaded pipe flanges attached to the outside of the box, 1 in. (2.5 cm) inside diameter (i.d.) threaded pipes were installed so that the ends of the pipes were flush with the interior surface of the insulation.

Description of Experimental Facilities

A forced-air cooler designed specifically for research by Baird et al. (1975) was used for this study. Air velocity, air temperature, relative humidity, container venting, and product stacking arrangement were important variables related to cooling biological materials that could be controlled. Temperature distribution within the individual product and within the product container, static pressure loss across the product container, and product moisture loss were among the parameters that could be measured during a test.

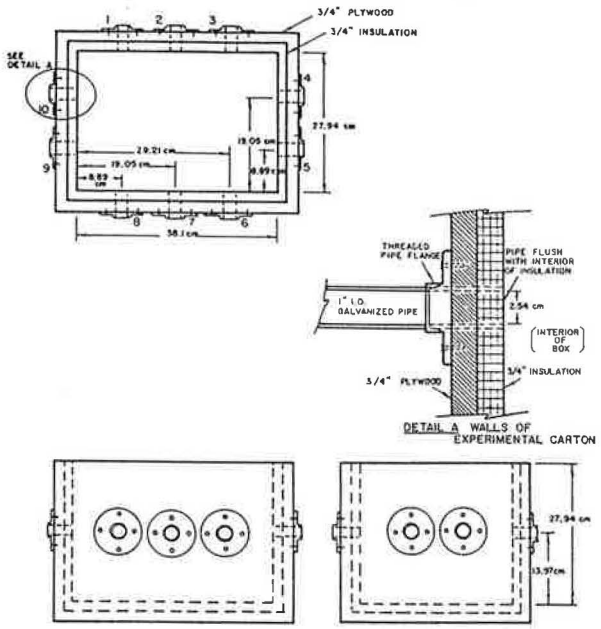

Figure 1 *The experimental orange carton*

Basic Construction of Precooler

Figure 2 shows the general location of the components and the air circulation diagram for the cooling facility. The product chamber was initially designed to accommodate a product load with maximum dimensions of 4 by 4 ft (1.2 by 1.2 m) cross section and 8 ft (2.5 m) high. This allowed cooling tests using pallet boxes or pallet loads. In order to study an individual carton, the product chamber was modified as shown in Figure 3 to accept the experimental orange carton mentioned above.

The location of the air-handling unit and airflow patterns is shown in Figures 2 and 3. To simulate the forced-air cooling of a carton of fruit, the experimental carton and the entrance plenum for this carton were securely fastened to the top of the product bin. As illustrated in Figure 3, the air entered the plenum of the experimental carton and underwent a 90° turn prior to entering one, two, or three 1-in. (2.5 cm) i.d. inlet holes. The air passed through the product and exited through one, two, or three 1-in. (2.5 cm) i.d. outlet holes. Table 1 presents the inlet and outlet combinations evaluated during this study. The air then continued into the product chamber and through the precooler (Figure 2).

The airflow rate leaving the carton was measured through the use of a pressure differential flow element installed in a 1-in. (2.5 cm) i.d. pipe connected to the threaded pipe flanges attached to the outlet of the carton. The flow rate was determined as a function of the difference between velocity and static pressure, measured with an electronic differential pressure manometer. When more than one outlet was used, a hot-wire anemometer was used to measure the relative flow leaving each hole.

The damper in the top of the experimental carton plenum was used to bypass air for tests with low airflow rates through the product carton. At the start of a test, the experimental carton with the exit vents sealed was attached to the plenum. Cold air was circulated through the plenum for a few minutes until the desired entering air temperature was achieved at the entrance to the experimental carton. Then the desired exit vents were opened to start the test. The venting arrangements were obtained by the use of

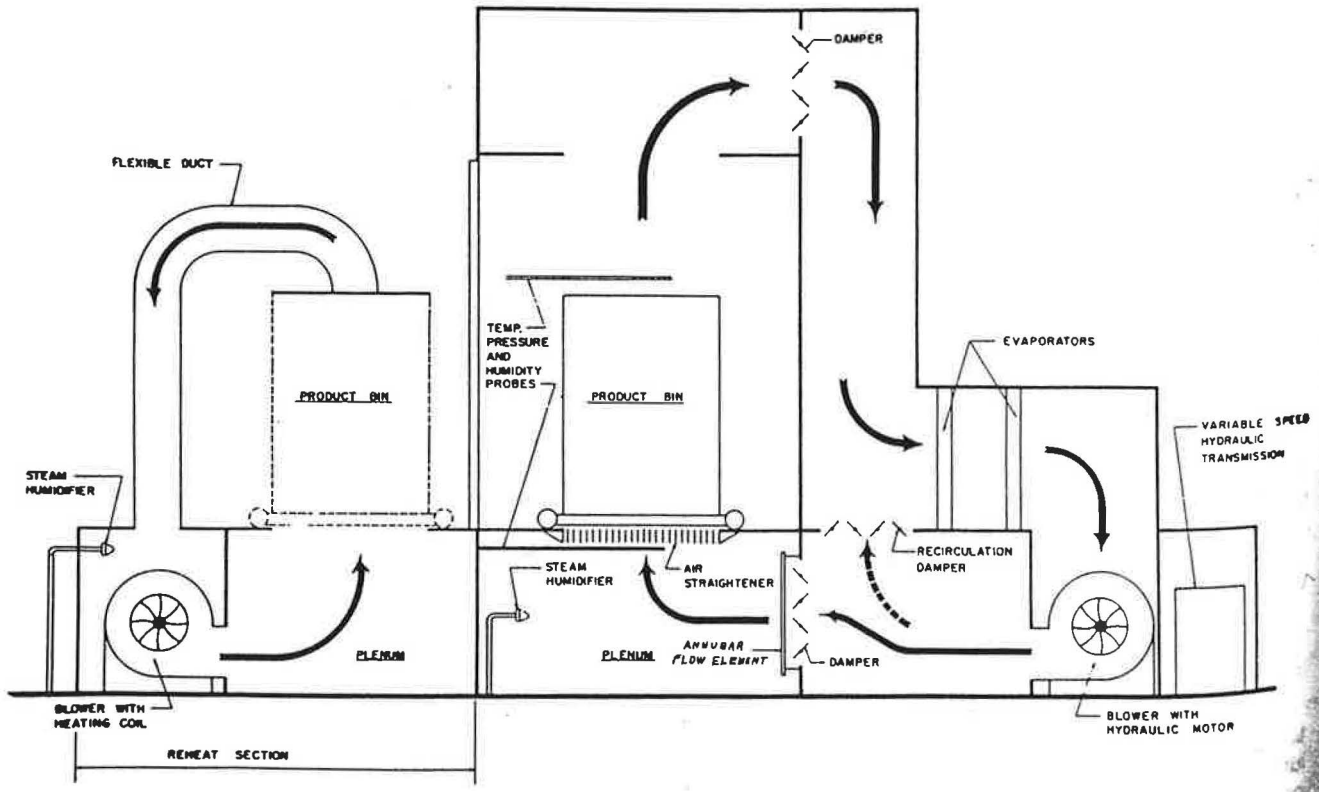

Figure 2 *Forced-air precooler components and air circulation diagram (Baird et al. 1975)*

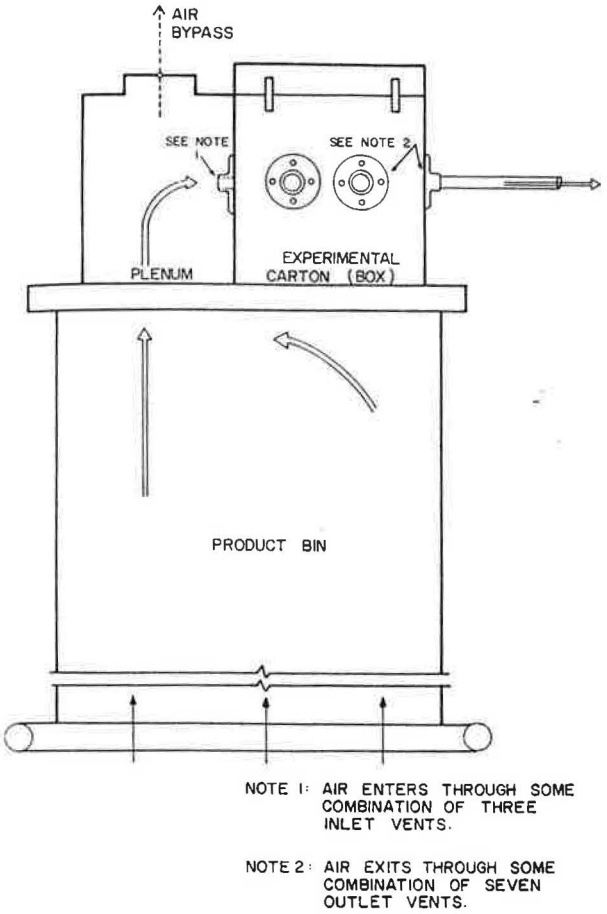

Figure 3 *Modification of product bin to accommodate experimental orange carton*

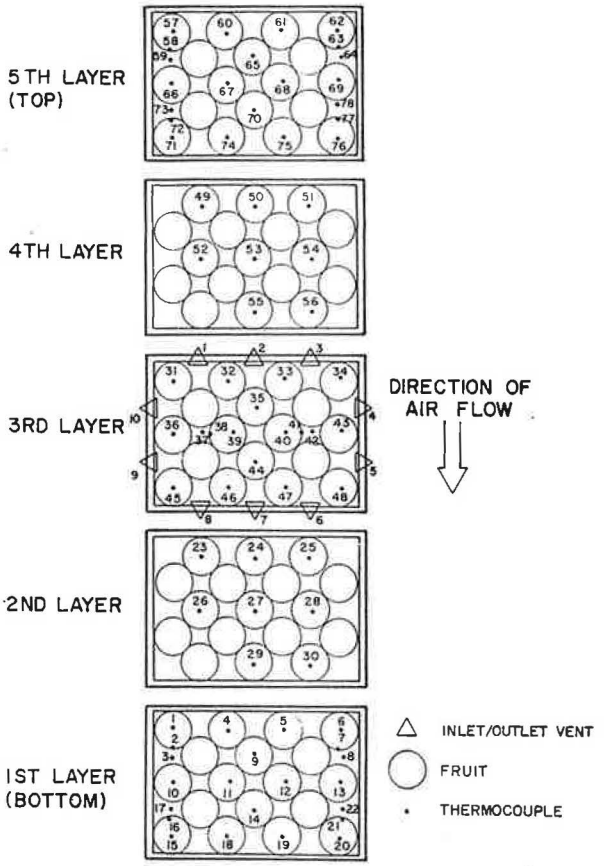

Figure 4 *Fruit and thermocouple locations in experimental orange carton*

rubber stoppers which were large enough to seal the pipes at the inlet or exit vent. The vent openings that were not needed for a particular test were plugged. A reheat section, as shown in Figure 2, was a self-contained unit placed adjacent to the product chamber so that a containerload of product was rolled out to heat the product to a predetermined uniform temperature before initial and repeated tests.

Experimental Test Procedures

Twelve tests were conducted with an experimental orange carton packed with 40 lb (18 kg) of size 100 Valencia oranges using airflow rates ranging from 2.6 to 43.6 cfm (1.6 by 10^{-3} to 2.6 by 10^{-2} m^3/s). These tests were conducted on six different venting arrangements with two flow rates for each. Considering the numbered vent locations shown in Figure 1, the flow patterns (boundary conditions) presented in Table 1 were evaluated. The airflow rates per vent arrangement, also shown in Table 1, are the flow rates through each of the inlet vents for a particular boundary condition. The total inlet flow rate for Boundary Condition 2 is twice the value reported in Table 1.

Each cooling test was conducted using 88 sized fruit which were weighed and placed into the experimental orange carton in a face-centered cubic packing arrangement, which Chau et al. (1983) reported as square-staggered. This stacking pattern resulted in five horizontal layers of fruit, with 18 fruit in the bottom, middle, and top layers and 17 fruit in the second and fourth layers. Thermocouples constructed from 36-gauge, insulated copper-constantan wire were placed at the center of 58 oranges and at the surface of 10 oranges. Ten thermocouples were also placed in the air spaces adjacent to the surface thermocouples to measure the air temperature within the orange carton. The locations of the thermocouples in each layer of the oranges are shown in Figure 4. Other temperature measurements included the entering and leaving air temperatures.

Temperature was recorded on a microprocessor-controlled data acquisition system capable of receiving 80 thermocouple inputs. Each thermocouple and other data inputs were read at 3-, 6-, 12-, or 15-minute intervals, based on the total length of the test run. A longer time interval was used for the lower flow rate tests. The oranges in the experimental carton were brought to a uniform temperature by the reheat section just prior to placement of the carton into the cooling chamber. The temperature of the cooling air entering the experimental carton was controlled at a constant temperature.

POROUS MEDIA FLOW ANALYSIS

After a literature review and temperature response data analysis, a three-dimensional finite element nonlinear porous media flow analysis was chosen for the problem under consideration. A general purpose commercial finite element analysis package (DeSalvo and Swanson 1983) was found to contain an option that allows the modeling of

TABLE 1
Boundary Condition Inlet and Outlet Air Vent Locations and Airflow Rates

Boundary Condition Number	Inlet Vents	Outlet Vents	Balanced Airflow Rate, cfm (m^3/s) per Each Inlet Vent (1)	(2)
1	2	7	3.3 (2.0 E-3)	21.3 (1.3 E-2)
2	1, 3	6, 8	3.3 (2.0 E-3)	9.3 (5.7 E-3)
3	1, 2, 3	6, 7, 8	2.6 (1.6 E-3)	12.9 (7.8 E-3)
4	2	4, 7, 10	11.2 (6.8 E-3)	43.6 (2.6 E-2)
5	2	7, 10	10.0 (6.0 E-3)	28.1 (1.7 E-2)
6	1	6	3.3 (2.0 E-3)	11.6 (7.0 E-3)

nonlinear, steady-state fluid flow through a porous medium, and appeared to be applicable to the case at hand.

Commercial Finite Element Package

A typical analysis consists of three phases: pre-processing (analysis definition), solution, and post-processing (interpretation of results).

The pre-processing phase is very important since the accuracy of the solution depends directly upon the degree of accuracy of the problem description. Input data prepared in the analysis definition would include the model description, boundary conditions, and the analysis type and options.

The model description involves creating the desired geometry, selection(s) from the element library, specification of geometric (real) constants describing properties of elements, and identification of material properties (e.g., viscosity, conductivity, and density). The user must ensure dimensional homogeneity.

The analysis is performed in the solution phase. For the nonlinear porous media flow case, this involves the solution of the matrix equation

$$[K]\{P\} = \{Q\} \tag{7}$$

where

$[K]$ = transmissivity matrix
$\{P\}$ = pressure vector (unknown)
$\{Q\}$ = mass flow rate vector

and the calculations of the pressure and mass flow distributions.

The porous media flow problem is formulated in a manner identical to that used for the thermal analysis, requiring only a change of variables to use thermal analysis to obtain a solution. Pressure is the variable rather than temperature. The momentum equation is simplified to

$$-(grad\ P) = Reff\ \overline{V} \tag{8}$$

where

$grad$ = gradient of a scalar function
P = pressure
$\overline{V}$ = seepage velocity vector

and

$$Reff = \mu/K + \beta\rho|\overline{V}| \tag{9}$$

where

μ = gas viscosity
K = absolute permeability of porous media
β = visco-inertial parameter
ρ = density.

Substituting Equation 8 into the continuity equation yields

$$\partial(k\partial P/\partial x)/\partial x + \partial(k\partial P/\partial y)/\partial y + \partial(k\partial P/\partial z)/\partial z = 0 \tag{10}$$

where $k = \rho/Reff$. Equation 10 is nonlinear because $Reff$ is a function of velocity. The coefficients of permeability, k, are (kx, ky, kz) internally calculated for each coordinate direction as

$$k = K\rho/(\mu + K\beta\rho|\overline{V}|) \tag{11}$$

Combining Equations 8 and 9 yields

$$-(grad\ P) = \mu\overline{V}/K + \beta\rho|\overline{V}|\ V \tag{12}$$

which is the same format as Equation 5. The solution results are evaluated in the third phase, where the user determines if the objective of the analysis was met.

This commercial package is available and useful for the type of analysis under consideration. Although straightforward, procedural familiarization is required during the analysis definition phase in selecting the geometry and elements, as well as specifying the input parameters and boundary conditions.

Verification of the commercial finite element package for porous media flow problems was obtained by calculation and comparison to previous published studies. The two-dimensional rectangular grain bin problem solved by Segerlind (1982), a three-dimensional grain bin problem solved by Khompis et al. (1984), and pressure drop as a function of air flow for oranges in bulk and in cartons solved by Chau et al. (1983) were modeled using the commercial package. The results were excellent, validating the commercial package for investigating pressure and velocity distributions in orange cartons.

Three-Dimensional Orange Carton

Use of porous media analysis to study air flows through a container of oranges presented several problems not encountered in previous studies. A primary concern was the overall scale of the porous media used in this case. This scale was finite when compared to semi-infinite cases studied by others. Because of the small dimension of the packing container, boundary (wall) effects could be significant. The wall contact with the fruit or vegetable presented two possible difficulties. The drag caused as the air passes the wall was one consideration. The second concern, which has been reported by other workers (Pillai 1977; Ridgway and Tarbuck 1968; Stanke and Eckert 1979), relates to the variance of the voidage or porosity adjacent to the walls when compared to the central portion of the porous media.

Pressure drops produced by the air inlets of packing containers were of concern when comparing the pressure drop through porous media (fruits or vegetables within the

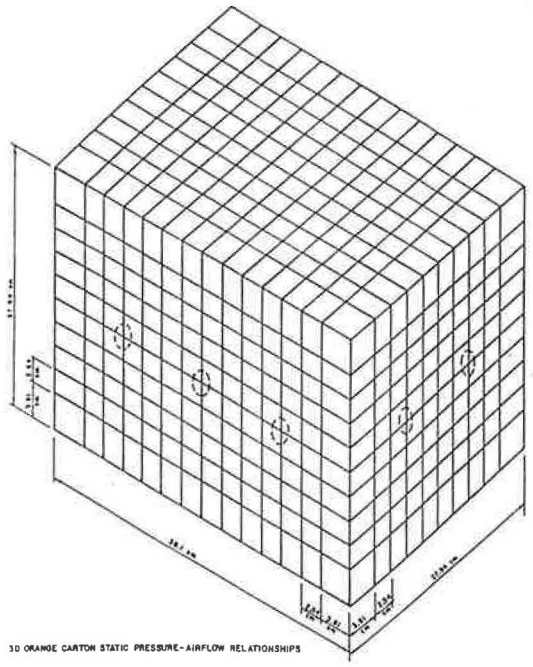

Figure 5 The node and element locations used to model a three-dimensional orange carton

cartons) to that of the pressure drop across the inlet(s) and exit(s).

Another consideration in cooling of fruits and vegetables was possible compaction during packing and subsequent shrinkage with time due to physiological changes and moisture loss. Porosity may change, for example, if the product becomes more compact due to shrinkage or handling. The porosity next to the inside top of the carton could increase, allowing more air to pass through this area.

Experimental results of Chau et al. (1983) were expanded to model an individual carton (Figure 1) packed with oranges. An eight-node, three-dimensional isoparametric thermal solid element, which allowed modeling of nonlinear steady-state flow through porous media, was used. The node and element locations are shown in Figure 5. The model consisted of 1815 nodes and 1400 elements. The first interior nodes were placed 1.5 in. (3.8 cm) from the walls, while the remaining interior nodes were placed every 1 in. (2.5 cm) along the axis of the experimental box. Larger node spacing near the wall was necessary due to the physical spacing of the vent openings.

Airflow rate boundary conditions used in the model were the same conditions used during the experimental temperature response study of size 100 square staggered packed oranges. The inlet/outlet locations and flow rates are shown in Table 1. Volume flow rates were converted to mass flow rates using air density for the inlet air temperature for a particular experimental test, 32° to 35°F (0° to 1.67°C). Boundary conditions were specified at nodal locations corresponding to the inlet and outlet vent locations. The airflow rate was specified at inlet(s) and the pressure was specified at the outlet(s). The no-flow or impermeable boundary condition, $\partial P/\partial n = 0$, was applied on solid boundaries where no pressure values were specified.

Input Coefficients

Input coefficients for the commercial finite element program are shown in Equation 9. Viscosity and density for air were taken from standard data tables. The absolute permeability of the porous media and the visco-inertial parameter were derived from experimental results.

Chau et al. (1983) presented a variation of the Ergun equation as

$$\Delta P/h = K_1 \mu V_s (1 - \epsilon)^2 / D_p^2 \epsilon^3 g_c + K_2 \rho V_s^2 (1 - \epsilon)/D_p \epsilon^3 g_c \quad (13)$$

Equation 13 is analogous to Equation 3. Comparing Equation 13 and Equations 8 and 9, the absolute permeability of the porous medium, K, and the visco-inertial parameter, β, is given by

$$1/K = K_1[(1 - \epsilon)^2/D_p^2 \epsilon^3] \quad (14)$$

and

$$\beta = K_2[(1 - \epsilon)/D_p \epsilon^3] \quad (15)$$

Chau et al. (1983) determined K_1 and K_2 by fitting experimental data and reported all the parameters required to solve Equations 14 and 15 for bulk-packed oranges. For size 100 oranges arranged in a square-staggered stacking pattern, the following values were reported:

$D_p = 0.245$ ft (0.0735 m); $\epsilon = 0.405$; $K_1 = 1566$; and $K_2 = 2.22$.

Air viscosity and density were assumed constant during the cooling process, and were evaluated at an average cooling test temperature of 50°F (10°C)

$\mu = 1.2$ by 10^{-5} lb/ft-sec (1.8 by 10^{-5} kg/m-sec);

and

$\rho = 7.7$ by 10^{-2} lb/ft^3 (1.2 kg/m^3).

Variable Porosity The commercial program calculated temperature response using constant porosity and input parameters specified above. A comparison of calculated temperature response with the corresponding experimental response indicated poor agreement. Predicted temperatures were warmer in regions adjacent to the walls of the container and slightly cooler in the central portion of the container away from the walls. The effect of the variation of the voidage or porosity adjacent to the walls was a major factor resulting in the poor fit of the experimental temperature response. Therefore, the model was modified to incorporate the effect of variable porosity.

The variation of the porosity as a function of distance from the interior wall of a three-dimensional carton packed with oranges is a subject requiring additional research. Ridgway and Tarbuck (1968) reported variation in porosity of large random beds to about five particle diameters from the wall. Pillai (1977) indicated variation in porosity up to three particle diameters from the wall for two-dimensional randomly packed beds, but that constant porosity beyond one particle diameter would result in less than 10% error. For the current study, calculation of the porosity adjacent to the walls of the carton was possible using basic geometric relationships and numerical integration. The variable porosity was calculated within the regions occupied by the finite elements adjacent to all six interior walls of the experimental orange carton. The element size adjacent to the wall was approximately half the diameter of an orange. The oranges were assumed to be

TABLE 2
Summary of Variable Porosity and Input Data

Element Location	Number of Elements	Porosity ϵ	K ft^2	K (m^2)	β ft^{-1}	β (m^{-1})
Center	800	0.32	2.6 E-6	(2.4 E-7)	192.3	(641.1)
Corners	8	0.44	1.0 E-5	(9.2 E-7)	60.3	(200.9)
Edges	112	0.58	4.2 E-5	(3.7 E-6)	19.8	(66.0)
4 Surfaces (27.9 by 38.1 cm)	384	0.52	2.3 E-5	(2.1 E-6)	30.8	(102.7)
2 Surfaces (27.9 by 27.9 cm)	128	0.52	2.5 E-5	(2.3 E-6)	29.2	(97.2)

perfect spheres. The volume of the oranges or portion of an orange lying within the elements adjacent to the walls was calculated. The porosity was defined in Equation 3 as the ratio of the void volume to total volume. The total volume was the calculated volume of the elements adjacent to the walls. The void volume was calculated by subtracting the volume of the oranges from the volume of the elements. Since the overall constant porosity used did not change, the porosity of the remaining 800 elements in the central portion of the carton was reduced to correspond to the increase in the porosity of the elements adjacent to the walls. The porosity of the different element types is shown in Table 2.

The commercial program has the capability of assigning individual material properties (β, K, etc.) to each individual element. Therefore, Equations 14 and 15 were solved based on the porosity for each of the selected groups of elements considered and using the values of D_p, K_1, and K_2 specified above. The results of these calculations for β and K are shown in Table 2.

Output Data Reorganization

The porous media analysis output provided the total velocity (magnitude of the velocity vector) and the three components of the velocity vector at the centroid of each element (Figure 6), in addition to the element volume and pressure gradient. To obtain the necessary data for the heat transfer model, the output was reorganized. This was accomplished with the post-processor and three FORTRAN programs. The post-processor was used to select, sort, and perform several mathematical operations on the element output information.

The first FORTRAN program calculated the component mass flow rates at the centroid of each element by multiplying the component velocity at the centroid by the density of the air and the area of the face normal to the velocity component. The area was calculated by dividing the element volume by the element dimension in the direction of flow. The heat transfer coefficient for each element, discussed below, was also calculated using the total velocity.

The second program calculated the mass flow rate across an element face by averaging the values of the mass flow rate at the centroids of the elements sharing the face. This was performed for each of the three component axes. For faces that were adjacent to the orange carton walls, the mass flow rate was of course zero except at inlet(s) or outlet(s).

The third program calculated the flow rates into each element. The flow could enter from any of six faces. For example, the flow into a particular element could be from both the positive and negative x-axis faces. In addition, the program created an identification procedure such that the entering temperatures were logically identified and correlated with the corresponding mass flow rate from the source element. This identification variable was necessary because the temperature leaving each element varied as a function of time.

The model was used to solve the 12 orange carton airflow boundary conditions presented in Table 1. The output from the model solution was available in a tabular report-type printout, user-specified output selection, and various graphical plots.

HEAT TRANSFER MODEL

Selection of a Model

The literature contains many citations of heat and mass transfer models. The approach of this study was to use two validated heat transfer models together to calculate the temperature response using the flow model results. The one-dimensional explicit finite difference numerical model for individual fruit using heat transfer equations for a homogeneous sphere without heat sources reported by Baird and Gaffney (1976) was used without major changes. The numerical model to predict temperature distribution within bulk loads of products (bed model), also reported

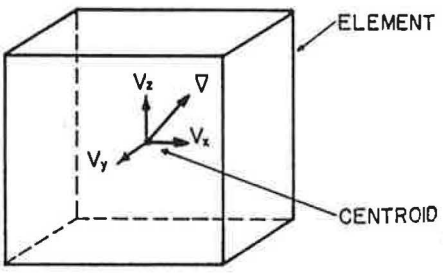

VELOCITY VECTOR AND THREE COMPONENTS

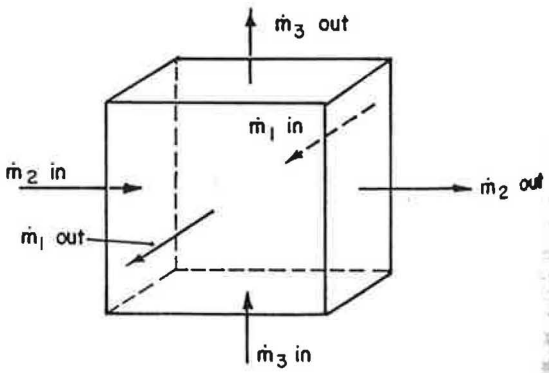

AIR FLOW RATE IN AND OUT

Figure 6 *Typical three-dimensional element showing velocity at centroid and air flow across element faces*

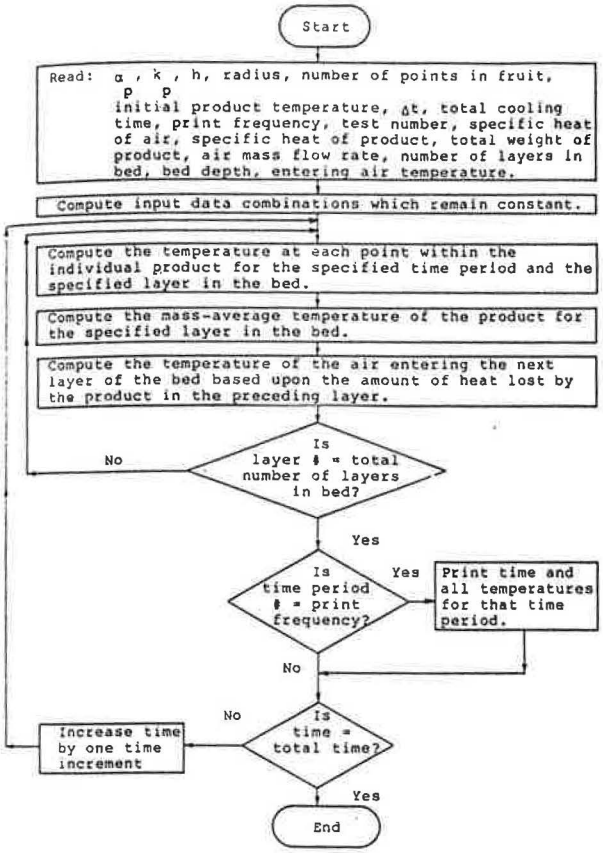

Figure 7 Flow diagram for the computer program to solve orange carton heat transfer equations

by Baird and Gaffney (1976), was modified for the current study.

Heat Transfer Model Modifications

Each three-dimensional element defined by the porous media flow analysis was treated like an individual bed similar to the bed model reported by Baird and Gaffney (1976). Air flow for the Baird and Gaffney (1976) bed model was one-dimensional or plug flow, while for the porous media flow analysis the air flow was three-dimensional. A typical three-dimensional element is shown in Figure 6. The airflow rate in or out of each face of the element was determined from data provided by the flow model.

To determine the temperature of the air entering a particular element from adjacent elements (or inlet boundary condition) the enthalpy entering each face of the element was used. Assuming ideal mixing and neglecting variation of air density and specific heat, the resulting temperature from the mixture was calculated from

$$\dot{m}_1 T_1 + \dot{m}_2 T_2 + \dot{m}_3 T_3 = \dot{m}_t T_m \qquad (16)$$

where

$\dot{m}_1, \dot{m}_2, \dot{m}_3$ = airflow rates entering element through faces 1, 2, and 3, respectively

T_1, T_2, T_3 = temperature of air entering element through faces 1, 2, and 3, respectively

$\dot{m}_t$ = total airflow rate entering element, $\dot{m}_1 + \dot{m}_2 + \dot{m}_3$

T_m = temperature as a result of perfect mixing.

Equation 16 was rearranged in terms of T_m to give

$$T_m = (\dot{m}_1 T_1 + \dot{m}_2 T_2 + \dot{m}_3 T_3)/\dot{m}_t \qquad (17)$$

T_m was used as the entering air temperature for the individual fruit model.

Convective Heat Transfer Coefficient

The convective heat transfer coefficient, h, was obtained from Baird and Gaffney (1976), who presented an "effective heat transfer coefficient" as

$$h = 1.17\,(k_a/D)\,[\rho_a V_a D/\mu_a]^{0.529} \qquad (18)$$

The velocity, V_a, in Equation 18 was defined as the superficial velocity. The best representative velocity for determining the convective coefficient from the model was identified as the calculated velocity at the centroid of the element. This velocity was defined as the superficial velocity by Ergun (1952). The magnitude of the centroidal velocity vector, $|\overline{V}|$, was substituted for V_a in Equation 18 and provided the following relationship for determining the convective heat transfer coefficient in terms of the velocity at the centroid of the element:

$$h = 1.17\,(k_a/D)\,[\rho_a|\overline{V}|\,D/\mu_a]^{0.529} \qquad (19)$$

Using the individual fruit model, the temperature at each point within the individual product for the specified period and element was calculated using the convective heat transfer coefficient (Equation 19) and the entering air temperature (Equation 17).

The final step consisted of calculating the temperature of the air leaving the element. This was accomplished by an analysis similar to the bed model used by Baird and Gaffney (1976). The change in the energy of the air as it moved through the element (control volume) was equal to the change in the internal energy of the product within the element

$$\dot{m}_t c_a\,(\partial T_m/\partial v)\,dv\,dt = -\rho_p c_p\,(\partial T_p/\partial t)\,dt\,dv_p \qquad (20)$$

where

T_a, T_p = temperature of the air and product, respectively

A = cross-sectional area of the packed bed

ρ_a, ρ_p = density of air and bulk density of product, respectively

c_a, c_p = specific heat of air and specific heat of product, respectively

t = time

v, v_p = volume of the element and volume of the product, respectively.

The volume of the product is related to the volume of the element by the porosity, ϵ,

$$v_p = (1 - \epsilon)v \qquad (21)$$

Inserting Equation 21 for the product volume in the energy balance above and solving for the change in air temperature resulted in

$$\partial T_m/\partial v = -(1 - \epsilon)\,[\rho_p c_p/\dot{m}_t c_a]\,\partial T_p/\partial t \qquad (22)$$

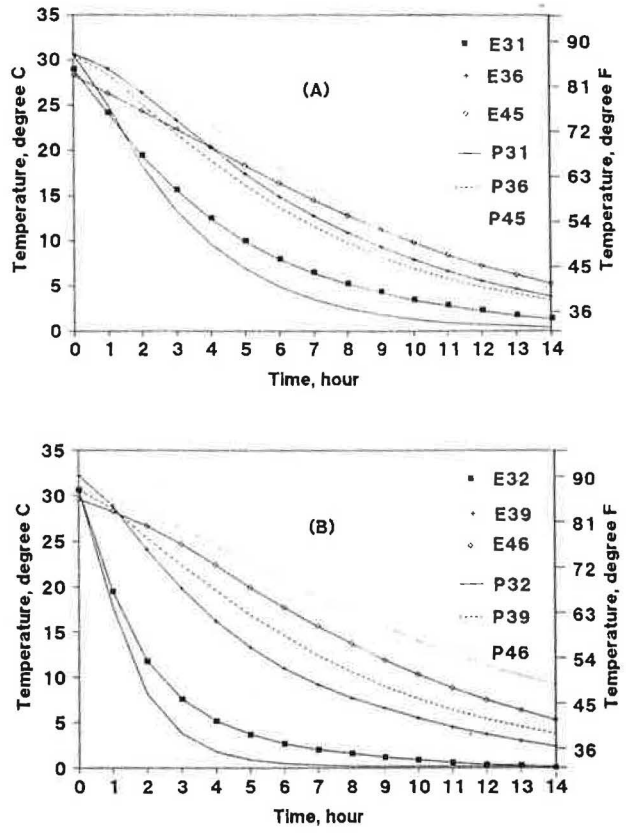

Figure 8 *Predicted (P) vs. experimental (E) data for Boundary Condition 1-1, third layer, thermocouples: (a) 31, 36, and 45; and (b) 32, 39, and 46*

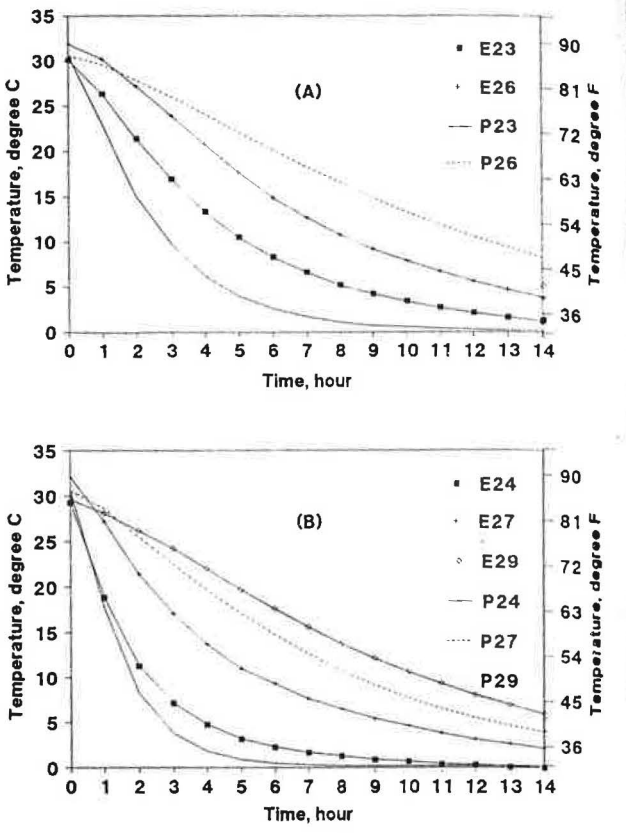

Figure 9 *Predicted (P) vs. experimental (E) data for Boundary Condition 1-1, second layer, thermocouples: (a) 23 and 26; and (b) 24, 27, and 29*

By considering the differential control volume (element) to be a finite volume, Equation 22 was approximated by

$$\Delta T_m/\Delta v = -(1-\epsilon)\,[\rho_p\, c_p/\dot{m}_t\, c_a]\,\Delta T_p/\Delta t \qquad (23)$$

The temperature leaving each face of an element was determined from the air temperature change calculated using Equation 23, and the value of the air temperature that entered the element was calculated using Equation 17. Then the procedure was repeated for the next element. The flow diagram for the computer program used to solve for the temperature response for the individual fruit model and Equation 23 is shown in Figure 7.

Heat Transfer Program

A fourth FORTRAN program was written to solve the heat transfer model, outlined by the flow chart procedures presented in Figure 7, using the reorganized flow model results. The physical and thermal properties of size 100 Valencia oranges reported by Gaffney and Baird (1980) were used for individual and modified bed models. For the vent locations used on the experimental carton, the flow model results were symmetric top and bottom. Therefore, only the bottom 700 elements were used in the heat transfer program in order to reduce the number of calculations required.

Temperature Response Data Reorganization

A FORTRAN program was written to reorganize the calculated temperature response so that the thermocouple locations in the model corresponded as closely as possible to the experimental thermocouple locations. The 78 thermocouple locations were assigned an air, product surface, or center time-dependent temperature value using the temperature value for a particular set of elements from the 700 elements available. The thermocouple location within the model corresponded with the physical location in the experimental carton.

Experimental vs. Predicted Temperature Response

Boundary Condition 1-1 was selected for presentation from the 12 boundary conditions shown in Table 1. This boundary condition provided a good test for the model because of the low flow rate and restrictive single inlet and exit locations.

Six thermocouples from the first and third layers and five thermocouples from the second layer (Figure 4) were selected for direct comparison of temperature response curves of predicted vs. experimental data. For each layer, two sets of two or three thermocouples were selected parallel to a line from inlet to exit. One set of thermocouples was located near the side of the carton and the other set was near the center of the carton. For the left side of the third layer, thermocouples 31, 36, and 45, and 32, 39, and 46 were selected and plotted in Figure 8. For the left side of the second layer, thermocouples 23 and 26, and 24, 27,

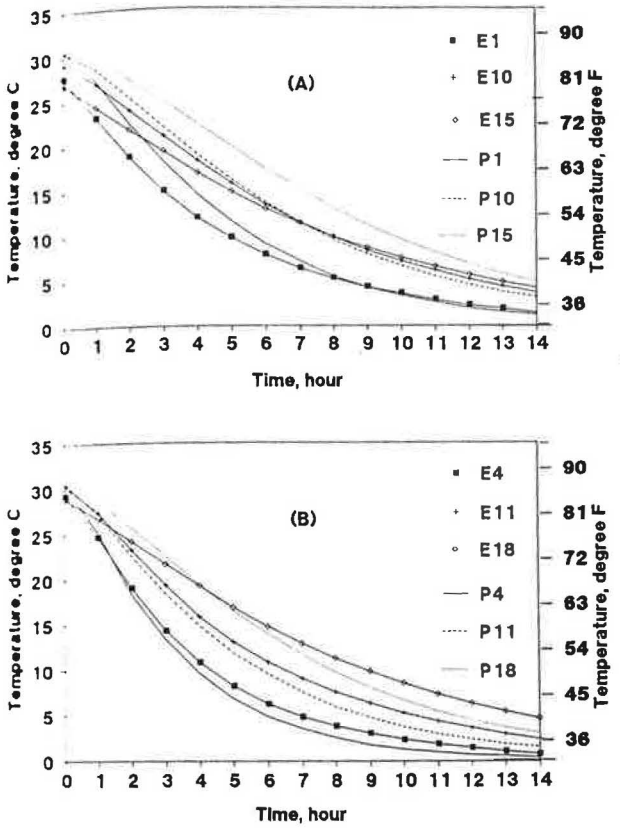

Figure 10 *Predicted (P) vs. experimental (E) data for Boundary Condition 1-1, first layer, thermocouples: (a) 1, 10, and 15; and (b) 4, 11, and 18*

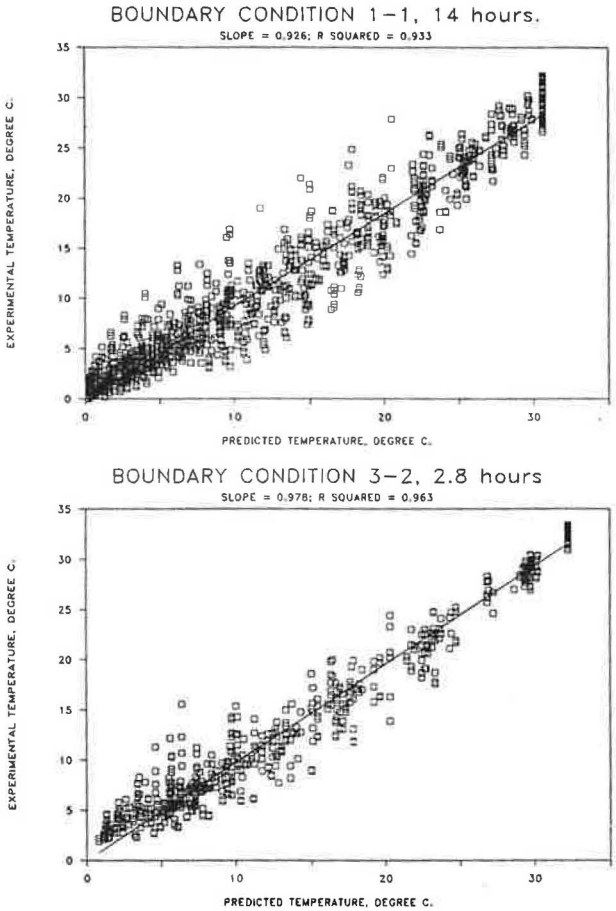

Figure 11 *Regression plot of the predicted temperature vs. the experimental temperature for Boundary Conditions: (a) 1-1 and (b) 3-2*

and 29 were selected and plotted in Figure 9. For the left side of the bottom layer, thermocouples 1, 10, and 15, and 4, 11, and 18 were selected and plotted in Figure 10.

In order to consolidate the large amount of data for each test into a more compact presentation, a regression plot of the predicted temperature vs. the experimental temperature was formed for each thermocouple location for the entire cooling test time. Center, surface, and air temperatures were all considered. For Boundary Condition 1-1, with a cooling test time of 14 hours, and Boundary Condition 3-2, with a cooling test time of 2.8 hours, the regression plots are presented in Figure 11.

DISCUSSION

Several trends exhibited by all 12 boundary conditions are evident in Figures 8 through 10. The first trend indicated that the experimental and predicted cooling responses fit better for oranges near the walls of the carton (regions with increased porosity) than for oranges in the center or core of the carton. The oranges in regions with least exposure to increased variable porosity exhibited a slower predicted vs. experimental temperature response. In Figure 8a, for the corner thermocouple 31 and side thermocouple 36 in the left half of the third layer of oranges, the predicted data indicated more cooling than the experimental data. In Figure 8b, the same trend applied for thermocouple 32 near the inlet vent, while the experimental data indicated a faster cooling rate than the predicted data for thermocouples 39 and 46. The difference between predicted and experimental temperature responses for thermocouples 32, 39, and 46 illustrates a second general trend, an increasingly poor fit of the experimental temperature response as the distance from the air inlet increased for oranges near the center of the carton.

In Figure 9, the predicted response was lower than experimental data for thermocouples 23 and 24, which were in the second layer of oranges adjacent to the inlet carton. This was also a general trend. The predicted vs. experimental data for second-layer thermocouples 26 and 27 exhibited poor agreement. Thermocouple 26 was in the central portion of the carton near but not adjacent to the carton wall and thermocouple 27 was in the central portion of the carton, just below a line from the inlet to exit vent. Thermocouple 27 exhibited a better predicted to experimental data fit than thermocouple 26. Thermocouple 29 was adjacent to the outlet carton wall just below the outlet vent and the predicted and experimental data were in close agreement.

In Figure 10a, thermocouples 1, 10, and 15 are adjacent to the bottom and the left side of the orange carton. As expected, the predicted and experimental temperature responses indicate that the predicted data would have cooled faster if not for the lower initial experimental temperatures. The predicted and experimental temperature responses of thermocouples 4, 11, and 18 in Figure 10b also indicate a lower predicted than experimental temperature response.

In regions where the porosity was increased (one-half orange diameter from the interior walls), the predicted temperature curves were generally lower than the experimental temperature curves. This is logical since more cooling air would pass through this region. In the regions where the porosity was constant, the predicted temperature curves were generally higher than the experimental cooling curves. In addition, in areas close to the increased porosity areas, the fit was worse than in areas close to the core of the oranges in the carton. This indicates that the variable porosity should be extended a further distance from the interior walls toward the center.

In Figure 11, the regression plot of the predicted temperature vs. the experimental temperature illustrates that the predicted data underestimated the cooling response of the oranges in the experimental carton. If the predicted and experimental data were identical, the data fitting line would have a slope of 1.0, while the actual data exhibited a slope of 0.93 and 0.96 for Boundary Conditions 1-1 and 3-2, respectively.

Experimental Error

Although the equipment and procedures used to measure the experimental temperature response have been developed and improved over several years, numerous factors directly affect the final temperature measurement. The instrumentation accuracy, the control of the airflow rate, the control of the inlet air temperature, the precise location of the thermocouples, the size and shape of the oranges, and the uniformity of packing the oranges are but a few of the many variables that have a direct bearing on the final temperature readings. Considering these and other factors, the temperature readings are estimated to be within ±2°F (1.1°C).

The initial temperature was obtained by reheating the carton of oranges as packed with thermocouples in place. Although it was possible to apply heat until the oranges were at almost the same steady-state temperature, the amount of time required to accomplish this was excessive in terms of productivity as well as physiological maintenance of the oranges. Deteriorated oranges required the entire orange carton to be emptied and filled with a new load of oranges that had been prepared with thermocouples. The heat transfer model required an initial product temperature and the average initial experimental temperature was used as the initial boundary condition since the temperature of only 58 of the 88 oranges was known. The standard deviation was such that the experimental and model thermocouple initial temperatures could be slightly different, up to 6°F (3.3°C). This altered the cooling curve of the model and produced a poorer comparison of experimental to model data (Figure 10a).

Convective Heat Transfer Coefficient

The convective heat transfer coefficient reported by Baird and Gaffney (1976) for cooling of oranges in beds was used in this study. This coefficient appeared to be satisfactory for the accomplishment of the current project objectives. In order to investigate the sensitivity of the model, one test was evaluated with the convective heat transfer coefficient halved and another with the coefficient doubled. The model was very sensitive to this forced change. Extension of this study could lead to an improved convective heat transfer coefficient.

Variable Porosity

Preliminary evaluation of the model did not apply variable porosity, and fit of the experimental data was very poor. A method for determining and applying the variable porosity was developed and this improved the fit of the predicted temperature response to that of the experimental temperature response. The results indicate the distance of penetration from the wall of the variable porosity for oranges packed in a three-dimensional orange carton should be increased. Additional experimental work is needed to provide the necessary variable porosity data for various sizes and shapes of cartons, and with various product packing arrangements. Increased porosity due to compaction near the top of the container should also be addressed.

Approximate Model Thermocouple Location

Future efforts should be made to design the element size and grid location to allow the physical location of the thermocouples to coincide with the center of a single element. This would provide a more reliable method for comparing experimental and numerical temperature response.

CONCLUSIONS

This study involved the application of several existing procedures in a unique way. A commercial finite element solution package was used to determine the pressure and velocity distribution for air flow through porous media. This procedure was first verified by comparing the results from porous media analysis with the results from research related to pressure and velocity distributions for air flow through two- and three-dimensional grain bins. Based upon favorable results, the porous media technique was used to model pressure loss through oranges in bulk and oranges packed in simulated orange cartons. Again, favorable results led to the evaluation of pressure and velocity distributions of air flow through a three-dimensional orange carton using the finite element porous media flow analysis. However, the airflow field for the orange carton was not known and not readily measurable using current instrumentation. To verify the porous media analysis for this problem, an indirect method of comparison was developed. The experimental temperature was measured for 12 different test conditions for oranges packed in an experimental orange carton and cooled using an experimental cooling facility. The flow boundary conditions and rates used for the 12 tests were used as input data for the porous media flow model to calculate pressure and velocity distributions for the oranges packed in the experimental orange carton. The absolute permeability and the viscoinertial input parameters were calculated using experimentally determined Ergun product coefficients, orange diameter, and variable porosity. An existing heat transfer program was modified to incorporate the calculated velocity distribution and provided a predicted temperature response. Experimental and predicted temperature responses for the 12 tests were compared and this comparison was used to indirectly evaluate the flow information calculated by the porous media flow analysis. The porous media flow analysis was found to provide adequate infor-

...ation if variable porosity within the orange carton was considered, although several areas for improvement were noted. Together the porous media flow model and heat transfer model have the capability to solve the pressure and velocity distributions and temperature response for various combinations of carton size and shape; size, number, and location of vent holes; packing arrangement; size and shape of fruit or vegetable; airflow rate; and cooling temperature typically encountered in the field. The technique described provides a valuable tool for improving and designing systems for cooling fruits and vegetables in shipping containers.

BIBLIOGRAPHY

Baird, C.D., and Gaffney, J.J. 1976. "A numerical procedure for calculating heat transfer in bulk loads of fruits and vegetables." *ASHRAE Transactions*, Vol. 82, Part 2, pp. 525-540.

Baird, C.D.; Gaffney, J.J.; and Kinard, D.T. 1975. "Research facility for forced-air precooling of fruits and vegetables." *Transactions ASAE*, Vol. 18, Part 2, pp. 376-379.

Chau, K.V.; Gaffney, J.J.; Baird, C.D.; and Church, G.A., III. 1983. "Resistance to air flow of oranges in bulk and in cartons." ASAE Paper 83-6007.

Collins, R.E. 1961. *Flow of fluids through porous materials.* New York: Reinhold Publishing Corp.

DeSalvo, G.J., and Swanson, J.A. 1983. *ANSYS engineering analysis system user's manual.* Houston, PA: Swanson Analysis Systems, Inc.

Ergun, S. 1952. "Fluid flow through packed columns." *Chem. Engng. Progress*, Vol. 48, pp. 89-94.

Gaffney, J.J., and Baird, C.D. 1980. "Physical and thermal properties of Florida Valencia oranges and Marsh grapefruit as related to heat transfer." ASAE Paper 80-6011.

Haas, E.; Felsenstein, G.; Shitzer, A.; and Manor, G. 1976. "Factors affecting resistance to air flow through packed fresh fruit." *ASHRAE Transactions*, Vol. 82, Part 2, pp. 548-554.

Hardenburg, R.E.; Watada, A.E.; and Wang, C.Y. 1986. *The commercial storage of fruits, vegetables, and florist and nursery stocks.* U.S. Department of Agriculture, Agriculture Handbook 66 (revised).

Khompis, V.; Segerlind, L.J.; and Brook, R.J. 1984. "Pressure patterns in cylindrical grain storages." ASAE Paper 84-3011.

Muskat, M. 1946. *The flow of homogeneous fluids through porous media.* Ann Arbor, MI: J.W. Edwards, Inc.

Pal, K.K. 1977. "Voidage variation at the wall of a packed bed of spheres." *Chem. Engng. Science*, Vol. 32, pp. 59-61.

Ridgway, K., and Tarbuck, K.J. 1968. "Voidage fluctuations in randomly-packed beds of spheres adjacent to a containing wall." *Chem. Engng. Science*, Vol. 23, pp. 1147-1155.

Scheidegger, A.E. 1960. *The physics of flow through porous media.* Toronto: University of Toronto Press.

Segerlind, L.J. 1982. "Solving the nonlinear air flow equation." ASAE Paper 82-3017.

Shedd, C.K. 1953. "Resistance of grains and seed to air flow." *Agr. Engng.*, Vol. 34, pp. 616-618.

Stanke, V., and Eckert, E. 1979. "A study of the area porosity profiles in a bed of equal-diameter spheres confined by a plane." *Chem. Engng. Science*, Vol. 34, pp. 933-940.

Talbot, M.T. 1987. "Pressure and velocity distribution for air flow through fruits packed in shipping containers using porous media flow analysis." Ph.D. dissertation, University of Florida.

Wang, J.K., and Tunpun, K. 1969. "Forced air precooling of tomatoes in cartons." *Transactions ASAE*, Vol. 12, No. 6, pp. 804-806.

DISCUSSION

W.E. Stewart, Jr., Professor, University of Missouri-Kansas City, Independence: It appears that Ergun's equation, which predicts apparent velocities, boundary-layer effects due to walls and varying porosity, and varying heat transfer coefficients on the fruit products, would tend to be the reason for the variations between predicted and experimental results. An improved model would seem an appropriate change.

M.T. Talbot: Dr. Stewart, thank you for your question/comment. The model fit better in some regions than in other regions, as you pointed out. The boundary condition selected for reporting was more difficult than several others that produced better results. Preliminary investigations revealed no rough approach that would adequately predict the velocity distribution. One of the objectives of the study was to evaluate the feasibility of the porous media approach. The finite element approach has been used to predict flow and pressure patterns by other researchers. A second objective was to use a commercial finite element program, which was based on the Ergun Equation. The porosity at different areas (variable porosity) within the orange carton must be specified to obtain satisfactory results from the porous media model. For this study, the porosity was calculated for the region adjacent to the interior walls (increased). For the remainder of the model, the porosity was specified as a constant (lowered). If the latter porosity had been calculated and specified as a function of the distance from the interior wall of the carton, the model would have provided much improved results, which is a subject for future research. We feel the results are encouraging and that the model does have merit.

The paper addresses your concern in more detail. During my oral presentation, the failure of the light pointer prevented me from discussing in detail the difference between the predicted and the experimental results.